ELSEVIER

Catalysis Today 83 (2003) 247–255

CATALYSIS TODAY

www.elsevier.com/locate/cattod

Test results of a catalytically assisted combustor for a gas turbine

Yasushi Ozawa [a,*], Yoshihisa Tochihara [a], Noriyuki Mori [a], Isao Yuri [a], Junichi Sato [b], Koji Kagawa [b]

[a] *Central Research Institute of Electric Power Industry, 2-6-1 Nagasaka, Yokosuka, Kanagawa 240-0196, Japan*
[b] *The Kansai Electric Power Co., Inc., 3-11-20 Nakoji, Amagasaki, Hyogo 661-0974, Japan*

Received 1 May 2002; received in revised form 24 October 2002; accepted 18 March 2003

Abstract

A catalytically assisted ceramic combustor for a gas turbine was designed and tested to achieve low NO_x emissions. This combustor is composed of a burner and a ceramic liner. The burner consists of an annular preburner, six catalytic combustor segments and six premixing nozzles, which are arranged in parallel and alternately. In this combustor system, catalytic combustion temperature is controlled under 1000 °C, premixed gas is injected from the premixing nozzles to the catalytic combustion gas and lean premixed combustion over 1300 °C is carried out in the ceramic liner. This system was designed to avoid catalyst deactivation at high temperature and thermal shock fracture of the ceramic honeycomb monolith of the catalyst. A 1 MW class combustor was tested using LNG fuel. Firstly, NO_x emissions from the preburner were investigated under various pressure conditions. Secondly, two sets of honeycomb cell density catalysts and one set of thermally pretreated catalysts ware applied to the combustor, and combustion tests were carried out under various pressure conditions. As a result, it was found that the main source of NO_x was the preburner, and total NO_x emissions from the combustor were approximately 4 ppm (at 16% O_2) at an adiabatic combustion temperature of 1350 °C and combustor inlet pressure of 1.33 MPa.

Keywords: Catalytic combustion; Gas turbine; Natural gas; Nitrogen oxides; Ceramic combustor

1. Introduction

Combined cycle power plants and co-generation systems have come into widespread use recently because of their high thermal efficiency. However, the control of nitrogen oxides (NO_x) is important for these systems since it is necessary to reduce NO_x, which is generated in a gas turbine combustor, to meet stringent NO_x regulations. Although low NO_x, lean premixed combustors have now been commercialized, a selective catalytic reduction (SCR) system, which requires considerable capital, operating and maintenance costs, must be equipped in many cases.

As an ultra-low NO_x technology, studies of catalytic combustion for gas turbine combustors were started in the 1970s [1]. In this method, combustion is approximately completed by the catalytic and thermal reaction within the catalyst bed. As a result, the catalyst temperature rises over the combustor outlet gas temperature, so it is difficult to apply this method to recent high-temperature gas turbines. To develop a low NO_x combustor technology using catalytic combustion for high-temperature gas turbines, a joint R&D project by CRIEPI (Central Research Institute of Electric Power Industry) and KEPCO (The Kansai Electric Power Co., Inc.) was started in 1988. In this

* Corresponding author. Tel.: +81-46-856-2121; fax: +81-46-856-3346.
E-mail address: ozaway@criepi.denken.or.jp (Y. Ozawa).

0920-5861/$ – see front matter © 2003 Elsevier B.V. All rights reserved.
doi:10.1016/S0920-5861(03)00245-1

Nomenclature

CO	carbon monoxide emissions (dry) (ppm)
cpi	cells per square inch
cr	fuel conversion over catalyst $= ((V_a + V_f)(HC_{in} - UHC)/((V_a + V_f)HC_{in} - 2V_f \cdot UHC)) \times 100$ (%)
HC_{in}	inlet hydrocarbon concentration (dry) (ppm)
H_{lCO}	lower heating value of CO (J/kg)
H_{lf}	lower heating value of fuel (J/kg)
H_{lUHC}	lower heating value of UHC (J/kg)
M_{CO}	molecular weight of CO (kg/kmol)
M_f	molecular weight of fuel (kg/kmol)
M_g	molecular weight of exhaust (dry) (kg/kmol)
M_{UHC}	molecular weight of UHC (kg/kmol)
NO_x	nitrogen oxides emissions (dry) (ppm)
P.F.	pattern factor $= ((\text{peak } T_g - \text{mean } T_g)/(\text{peak } T_g - \text{mean } T_{bi})) \times 100$ (%)
P_g	combustor exit pressure (MPa)
P_i	inlet air pressure (MPa)
ΔP	combustor pressure loss $= ((P_i - P_g)/P_i) \times 100$ (%)
t	time on stream (h)
T_{ad}	adiabatic combustion temperature (°C)
T_{bi}	combustor inlet temperature (°C)
T_c	catalyst bed temperature (°C)
T_{ci}	catalyst inlet gas temperature (°C)
T_g	combustor exit gas temperature (°C)
UHC	unburned hydrocarbon emissions (dry) (ppm)
V_a	air flow rate (m^3_N/s)
V_f	fuel flow rate (m^3_N/s)
W_a	air flow rate (kg/s)
W_{fc}	fuel flow rate for catalyst (kg/s)
W_{fd}	fuel flow rate for preburner (kg/s)
W_{fp}	fuel flow rate for premixing nozzle (kg/s)
W_{ft}	total fuel flow rate (kg/s)
W_g	exhaust flow rate (dry) (kg/s)

Greek letter

η	combustion efficiency $= 100 - (W_g/(M_g \cdot W_{ft} \cdot H_{lf}) \times (CO \cdot M_{CO} \cdot H_{lCO} + UHC \cdot M_{UHC} \cdot H_{lUHC})) \times 10^{-4}$ (%)

work, to avoid thermal degradation of the catalyst at high temperature, a catalytically assisted combustor with a ceramic liner was designed and tested under atmospheric pressure [2]. Later, that with a metal liner was tested under high-pressure conditions [3], after which that with a ceramic liner was modified and tested under high-pressure conditions. This paper describes the test results of the combustor with a ceramic liner under high-pressure conditions.

2. Design of the combustor

Aiming to achieve the targets shown in Table 1, a 1 MW class combustor as shown in Fig. 1 was designed. The combustor is composed of a burner section and a premixed combustion section as described elsewhere [4]. The burner section consists of an annular preburner, six catalytic combustor segments and six premixing nozzles. Each catalytic combustor segment is composed of three fuel nozzles, three venturi mixers and a set of honeycomb catalysts. Three fuel nozzles are inserted in each premixing nozzle. There are six holes for injecting premixed gas into the catalytic combustion gas on both sides of the premixing nozzle exit. The catalyst segments and the premixing nozzles are arranged alternately to form a circle to ensure adequate mixing. Premixed combustion is made in a ceramic liner, which is composed of an outer metal wall, a ceramic fiber layer and inner ceramic tiles as described elsewhere [5]. In the premixed combustion section, an igniter is temporarily inserted to assist the smooth ignition of the premixed gas.

Air is heated by the preburner to the temperature that will enable the catalyst to maintain stable activity, and is distributed to the catalyst segments and premixing nozzles. Fuel is fed to the catalyst and to the premixing nozzles, and the premixed gas is injected into the catalytic combustion gas, and then recirculating flow occurs behind the end face of the premixing

Table 1
Targets for combustor performance

Combustor exit gas temperature (°C)	>1300
NO_x emissions (ppm)	<5 (16% O_2)
Combustion efficiency (%)	>99.9
Total pressure loss (%)	<5
P.F. (%)	<15

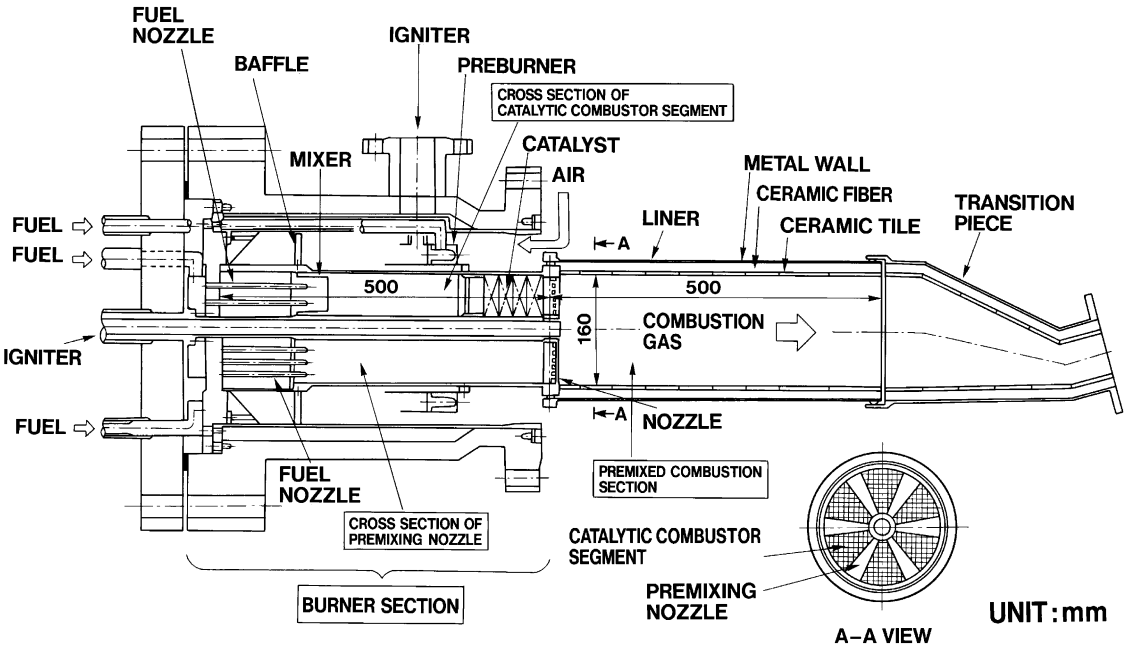

Fig. 1. Schematic of the combustor.

nozzles. As a result, lean premixed combustion over 1300 °C is stabilized by both the catalytic combustion gas and the recirculating flow. The cross-sectional area of the catalyst and air distribution were increased as much as possible to stabilize the premixed combustion at as low a catalyst temperature as possible. The fuel concentration for the catalyst was limited by the peak temperature of the catalyst bed. The fuel and air distribution to the premixing nozzle was determined based on combustion stability and the target maximum NO_x of 5 ppm (at 16% O_2). The liner cooling air was minimized by applying a ceramic liner to lower the NO_x emissions. The typical airflow split in this combustor is 65% for the catalysts, 30% for the premixing nozzles and 5% for the liner cooling, for the catalyst holders' cooling and for leaking. In case of the combustor with a metal liner designed to reduce NO_x emissions to 10 ppm (at 16% O_2) [3], the air flow split was 55% for the catalysts, 30% for the premixing nozzles and 15% for the liner cooling etc.

In order to avoid backfire into the premixing nozzle, the gas velocity in the nozzle was maximized within the pressure loss limitations, and the fuel concentration in the nozzle was also limited. This combustor was designed under the assumption that an air bypass valve [6] or another method of controlling combustion air was applied to maintain an adequate fuel/air ratio in the combustion area over a wide range of load.

These designs are expected to offer the following merits:

(1) The structural reliability of the ceramic monolith of the catalyst will be maintained since small catalysts can be applied.
(2) Premixed combustion downstream of the catalyst is stabilized with lower catalyst temperature.
(3) Keeping the catalyst temperature low will prevent deterioration of the catalysts.
(4) Stable combustion will be achieved under a wide range of combustor operating conditions since each fuel flow to the catalysts and the premixed combustion section can be properly controlled.

3. Catalyst

The Pd/Pt/Rh catalyst [7] shown in Table 2 was selected. Its major active ingredient is Pd, which is supported on a stabilized alumina washcoat on a honeycomb type monolith made of cordierite. Catalyst

Table 2
Catalyst properties

Substrate	Cordierite honeycomb monolith
Washcoat	Stabilized Al_2O_3 80 g/l + ZrO_2 20 g/l
Catalyst	Pd 20 g/l + Pt 5 g/l + Rh 2 g/l

configurations are shown in Fig. 2. In order to investigate the effect of the cell density of the catalyst on the combustion performance, two kinds of catalyst configurations were tested. Venturi mixers of wider internal diameter were installed at the inlet of the catalytic combustor segments for tests nos. 3 and 4 to offset the larger pressure loss of the catalyst set. In order to investigate the catalyst deactivation effect, a set of aged catalysts was also tested. The thermal aging was made by using an electric furnace in air flow for 1000 h at 750 °C, which was the mean temperature of the catalysts in the previous combustion test [3].

4. Test facility and conditions

Combustion tests were performed using high-pressure test facilities as described elsewhere [4]. Air from a compressor is heated with an indirectly fired heat exchanger and fed to a vessel in which the combustor is included. Air to the burner section through the preburner is distributed to catalytic combustion segments and premixing nozzles. Fuel from a tank of liquefied natural gas (LNG) is introduced to the preburner, the catalyst and the premixing nozzles, and is controlled individually. Combustor inlet temperature was measured at the preburner inlet and was approximately 10 °C lower than the combustion air temperature measured at the vessel inlet due to heat loss from the vessel. In the measurement duct, the combustion gas temperature is measured by 24 R-type thermocouples and emissions are sampled by two averaging sampling probes made of stainless steel and cooled by water. Emissions are analyzed by online gas analyzers. The catalyst bed temperatures are measured at the point 5 mm inside the bed outlet by 18 K-type thermocouples that are inserted and cemented into the catalyst cells. Table 3 shows the properties of the fuel sampled from the fuel line during the combustion test

Table 3
Fuel composition

Composition (vol.%)	Test no.			
	1	2	3	4
CH_4	82.8	83.6	80.4	72.9
C_2H_6	7.0	7.9	9.6	12.2
C_3H_8	5.8	5.6	6.6	10.0
i-C_4H_{10}	1.8	1.2	1.5	2.1
n-C_4H_{10}	2.5	1.6	1.9	2.7
i-C_5H_{12}	0.0	0.0	0.0	0.0
n-C_5H_{12}	0.0	0.0	0.0	0.0
N_2	0.1	0.1	0.0	0.1

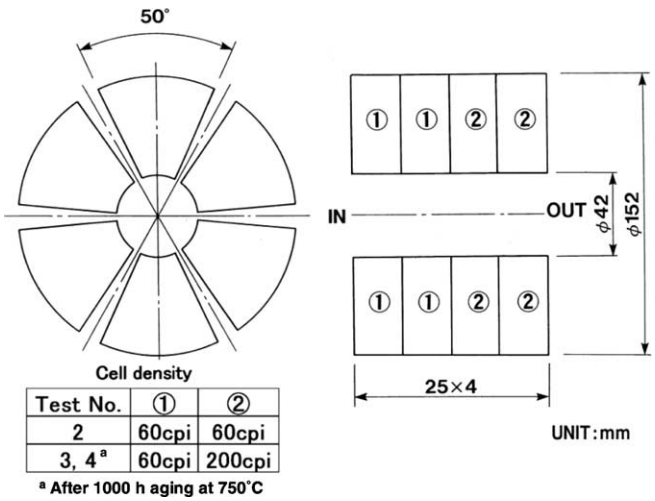

Fig. 2. Catalyst configurations.

Table 4
Base load conditions

Combustor inlet air pressure (MPa)	1.33
Air flow rate (kg/s)	2.60
Fuel flow rate (kg/s)	0.0690
GHSV[a] (h^{-1})	4.6×10^6
Combustor inlet temperature (°C)	370
Catalyst temperature (°C)	<1000
Combustor outlet gas temperature (°C)	1350

[a] Gas hourly space velocity (gas flow (m^3_N/h)/catalyst volume (m^3)).

and analyzed by TCD gas chromatography. The fuel composition somewhat varied in each test because light constituents in LNG gradually vaporized prior to heavy ones with time stored in the tank. Table 4 shows the test conditions at a base load. At this condition, catalyst inlet velocity is 25 m/s. The following combustion tests were performed:

Test no. 1 : A preburner test.
Test no. 2 : A combustor test using a set of 60 cpi catalysts.
Test no. 3 : A combustor test using a set of different cell density catalysts.
Test no. 4 : A combustor test using a set of aged catalysts.

The purpose of these changes is to estimate NO_x emissions from the preburner and the effect of catalyst temperature and catalyst deactivation on premixed combustion stability.

Catalytic combustion and premixed combustion were initiated under the conditions of 0.35 MPa, and then air and fuel were increased in proportion to the increasing pressure to investigate the effect of pressure under constant residence time. The pore volume, BET surface area, CO chemisorption and metal loading of the catalysts in test no. 4 were measured by an Autopore 9220 (Miromeritics), Gemini 2360, Model R-6015 (Okura Riken) and ICPS-2000 (Shimadzu), respectively.

5. Test results and discussions

5.1. Preburner performance

In test no. 1, fuel was fed only to the preburner, and the temperature distribution in the catalyst bed

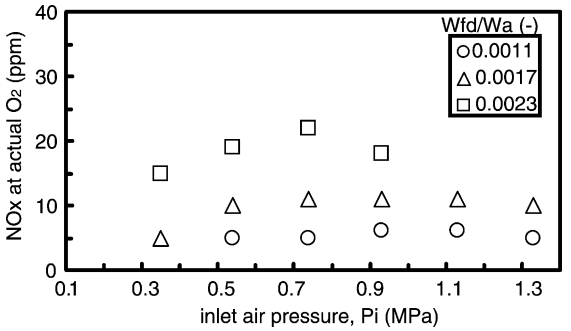

Fig. 3. Preburner NO_x emissions at combustor exit. Test conditions: $W_a/P_i = 1.95$ kg/(MPa s), $T_{bi} = 330$ (0.35 MPa)–370 °C (1.33 MPa).

and emissions at the combustor exit were measured under the same inlet conditions as the combustion test nos. 2–4. The largest difference among the temperatures measured by the 18 thermocouples was 30 °C. Due to the need to minimize the inlet temperature for the Pd/Pt/Rh catalyst, a mean temperature of 400 °C at the catalyst inlet proved to be necessary. Fig. 3 shows the NO_x emissions under various inlet pressures (P_i) and fuel/air ratios (W_{fd}/W_a), keeping the ratio of air flow rate to inlet air pressure (W_a/P_i) constant at 1.95 kg/(MPa s). NO_x emissions increased with increasing pressure up to 0.74 MPa, but were hardly affected by further pressure increases from 0.74 to 1.33 MPa. At the base load condition, W_{fd}/W_a was 0.001 and NO_x emissions were 5 ppm (at actual O_2). The combustion efficiency (η) was over 99% at all the test points.

5.2. Effect of pressure on combustor performance

Fuel was fed to the preburner, the catalyst and the premixing nozzles, and the effect of pressure on the combustion characteristics was examined in test nos. 2–4. P_i was increased while keeping W_a/P_i, catalyst inlet temperature (T_{ci}) and combustor exit gas temperature (T_g) constant. Fig. 4 shows the catalyst bed temperature (T_c). The mean temperature was 700 °C in test no. 2 and was 780 °C in test no. 3. This result indicates that the temperature increased with increasing cell density of the catalyst. The mean temperature in test no. 4 was 800 °C. One of the causes of the higher catalyst temperature in test no. 4 was thought to be the lower concentration of CH_4 in fuel

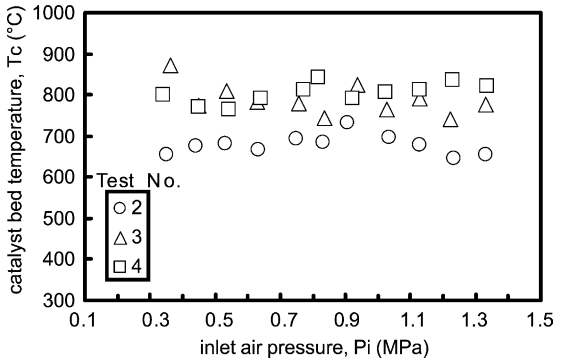

Fig. 4. Catalyst bed temperature on pressure change test. Test conditions: $W_a/P_i = 1.95$ kg/(MPa s), $T_{bi} = 330$ (0.35 MPa)–370 °C (1.33 MPa), $T_{ci} = 400$ °C, $T_g = 1350$–1380 °C.

than that used in the other tests (Table 3), which promoted the catalyst activity. These temperatures were lower than that of Pt/Pd catalyst reported by Kuper et al. [8] probably due to the lower cell density of the honeycomb monolith. Fig. 5 shows NO_x emissions and η at the combustor exit, and NO_x emissions from the preburner estimated by the preburner test results mentioned above. The data of NO_x emissions from the preburner (test no. 1) were fitted to a cubic function for each pressure condition and adapted to the operating conditions of the preburner in test nos. 2–4. NO_x emissions decreased with increasing P_i, 5 ppm (at 16% O_2) of the emissions was achieved over 0.9 MPa and at the base load condition it ranged from 3.7 to 4.1 ppm (at 16% O_2). NO_x emissions from the preburner also tended to decrease significantly with increasing P_i. Combustor inlet temperature (T_{bi}) increased from 330 to 370 °C with increasing P_i, so the fuel/air ratio of the preburner (W_{fd}/W_a) decreased with increasing P_i to control the catalyst inlet gas temperature at 400 °C. Changes in fuel distributions with pressure are shown in Fig. 6. The fuel distribution to the preburner (W_{fd}/W_{ft}) decreased with increasing P_i due to increase in the combustor inlet temperature. As a result, NO_x emissions from the preburner decreased with increasing P_i, which mainly affected the total NO_x emissions. Although Fig. 6 shows a small decrease of fuel distribution to the premixing nozzle (W_{fp}/W_{ft}) with increasing P_i, this effect on total NO_x emissions is much less than the preburner. This figure also shows that there is a region in which the NO_x emissions caused by the preburner are higher than the NO_x emissions at the combustor exit. This result indicates that the NO_x emissions from the preburner were reduced in the catalyst bed or in the premixed combustion section. η in test no. 2 is lower than that in test nos. 3 and 4, but was over 99.98% and stable combustion was maintained throughout the tests. There was little difference in the results between test nos. 3 and 4, so the effect of catalyst deactivation was not confirmed clearly. The pattern factor (P.F.) of the combustor exit gas was extremely low at less than 4%. Combustor pressure loss (ΔP) decreased with increasing pressure: 5% loss was achieved over 0.44 MPa and at the base load condition it was less than 4%.

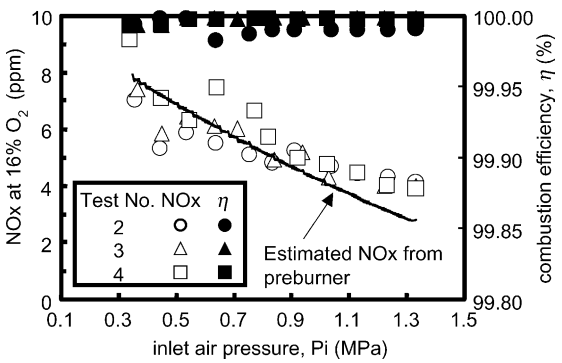

Fig. 5. Effect of pressure on NO_x emissions and combustion efficiency. Test conditions: same as in Fig. 4.

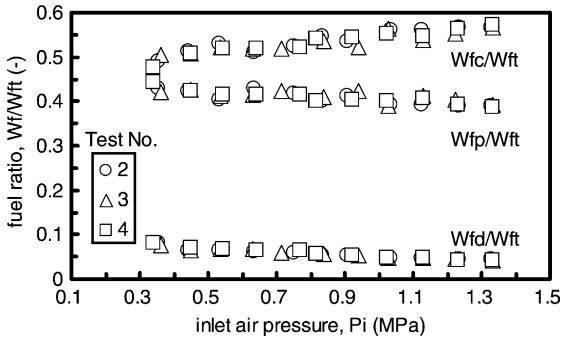

Fig. 6. Fuel distribution in pressure change test. Test conditions: same as in Fig. 4.

Fig. 7 shows the fuel conversion (cr) over the catalyst in test no. 4. In this test, fuel was fed only to the preburner and the catalyst, while the other conditions were the same as those of the above tests. The cr was approximately 30% and slightly decreased with

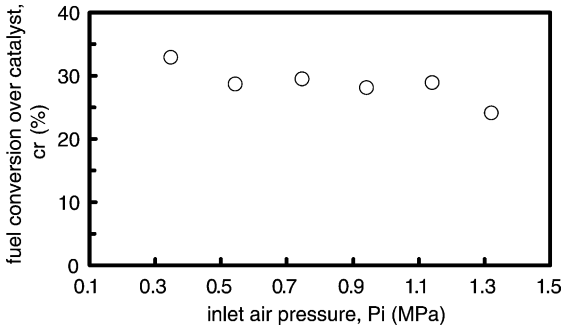

Fig. 7. Relation between pressure and fuel conversion over catalyst in test no. 4. Test conditions: $W_a/P_i = 1.95$ kg/(MPa s), $T_{bi} = 330$ (0.35 MPa)–370 °C (1.33 MPa), $T_{ci} = 400$ °C, $T_c = 790$–840 °C.

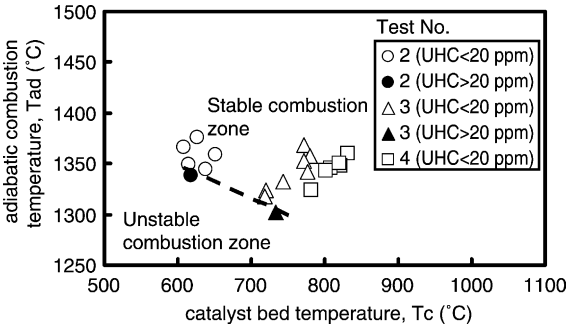

Fig. 9. Stable combustion zone. Test conditions: $P_i = 1.33$ MPa, $W_a = 2.60$ kg/s, $T_{bi} = 370$ °C, $T_{ci} = 400$ °C.

increasing pressure, which caused the increase of fuel distribution to the catalyst (W_{fc}/W_{ft}) shown in Fig. 6.

5.3. Combustion stability

Fig. 8 shows combustion stability for 2 h of combustion under the base load conditions in test no. 2. Stable combustion was carried out, and NO_x emissions and η were kept in the range from 4.1 to 4.4 ppm (at 16% O_2) and over 99.99%, respectively. At the base load condition, excess air ratio, which corresponds to an adiabatic combustion temperature (T_{ad}), was changed to estimate the combustion stability. Fig. 9 shows the effect of catalyst bed temperature (T_c) and adiabatic combustion temperature (T_{ad}) on combustion stability. 20 ppm (at actual O_2) of UHC emissions at the combustor exit was defined as the boundary condition between stable and unstable combustion. This figure indicates that T_c of over 750 °C was required for stable premixed combustion at 1350 °C with a safety margin. From this standpoint, the catalyst configuration of test nos. 3 and 4 was preferable to that of test no. 2. Dalla Betta et al. reported the results of kinetic model calculations showing fuel combustion in hot post-catalyst regions [9]. This report shows that CO is below 10 ppm within 4–5 ms at 1.22 MPa and 925 °C. In the case of our combustor, the catalyst temperature required to stabilize the post-catalyst combustion was much lower than this because a higher fuel concentration of premixed gas was injected into the catalytic combustion gas.

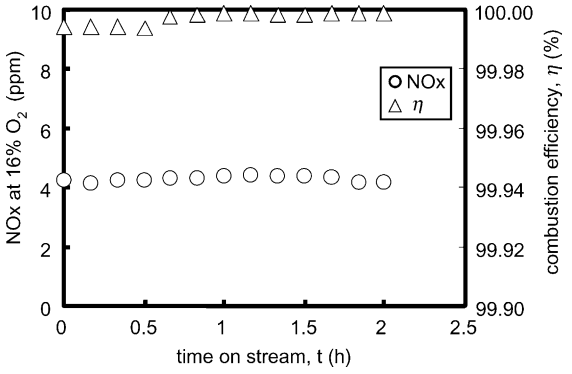

Fig. 8. Results of 2 h combustion in test no. 2. Test conditions: $P_i = 1.33$ MPa, $W_a = 2.60$ kg/s, $T_{bi} = 370$ °C, $T_{ci} = 400$ °C, $T_g = 1350$ °C.

5.4. Effect of oscillation of catalytic reaction

An oscillating behavior of the catalyst bed temperature was observed under all tested conditions. The mean period of oscillation was 35 s and the mean amplitude was 60 °C. On the other hand, the gas temperature and emissions at the combustor exit, both of which were continuously measured, were stable and little oscillating behavior was observed. The mean oscillation period of ΔP through the combustor was 35 s and the mean amplitude under the base load conditions was 0.8 kPa, which was affected by the oscillation of catalytic reaction, and the level was thought to be allowable. This level of oscillating behavior of the catalytic reaction is considered to affect only the premixed combustion characteristics under unstable leaner conditions.

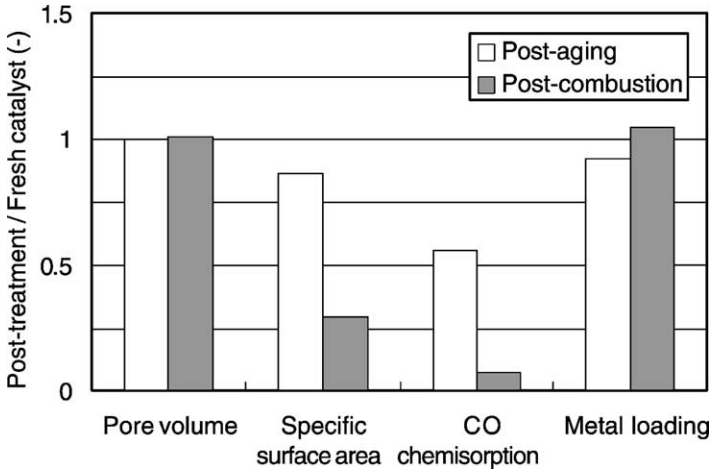

Fig. 10. Change in catalyst properties in test no. 4. Post-aging: catalyst after 1000 h aging at 750 °C. Post-combustion: 4th stage of catalyst after 1000 h aging at 750 °C and 5 h combustion testing at T_c of 800 °C.

5.5. Soundness of combustor and catalyst

The ceramic tile temperature of the ceramic liner rose over 1000 °C from the point of 280 mm from the exit of the burner section and the peak temperature was 1050 °C at the point of 460 mm. On the other hand, the metal wall temperature of the ceramic liner was kept at the same temperature as that of the combustion air. The total combustion time over 1300 °C was 20 h, and especially, that of the transition piece was about 40 h including a previous ceramic combustor test at 1500 °C [5]. The total reaction times of the catalyst sets over 650 °C ranged from 5 to 20 h. After the tests, the combustor components were visually inspected and no damage was detected. Fig. 10 shows the changes in catalyst properties in test no. 4. The pore volume and the metal loading were scarcely changed by thermal aging and combustion testing, but the specific surface area and CO chemisorption were decreased. Especially, the decreases by the combustion test were larger than those by the thermal aging. The main cause was thought to be that the catalyst temperature in the combustion test was higher than that in the thermal aging. One of the reasons why there was little difference in the results between test nos. 3 and 4 was considered to be that the catalyst activity was not decreased significantly by the thermal aging.

6. Conclusions

A catalytic combustor combined with premixed combustion was designed and tested at high pressures. As a result, it was found that the main source of NO_x was the preburner, and total NO_x emissions were approximately 4 ppm (at 16% O_2) at an adiabatic combustion temperature of 1350 °C. Low NO_x combustion was achieved with the assistance of catalytic combustion that stabilized lean premixed combustion and due to the ceramic liner that needed less cooling air. The catalyst temperature required to stabilize the post-catalyst combustion was over 750 °C. The effect of catalyst deactivation was not confirmed clearly because of the fluctuations of fuel composition and small amount of the catalyst deactivation by the thermal aging.

Acknowledgements

The authors sincerely thank Mr. S. Kikumoto, Mr. K. Sagimori and Mr. T. Kanazawa of KEPCO and Dr. T. Abe, Dr. T. Hisamatsu and Dr. T. Fujii of CRIEPI, who helped us in promoting this research project, and Dr. T. Inui and Dr. H. Fukuzawa, who helped us in developing the catalyst.

References

[1] W.C. Pfefferle, R.V. Carrubba, R.M. Heck, G.W. Roberts, ASME Paper No. 75-WA/FU-1.
[2] Y. Ozawa, J. Hirano, M. Sato, M. Saiga, S. Watanabe, Trans. ASME J. Eng. Gas Turb. Power 116 (1994) 511.
[3] Y. Ozawa, T. Fujii, M. Sato, T. Kanazawa, H. Inoue, Catal. Today 47 (1999) 399.
[4] Y. Ozawa, Y. Tochihara, N. Mori, I. Yuri, T. Kanazawa, K. Sagimori, Trans. ASME J. Eng. Gas Turb. Power 121 (1999) 422.
[5] I. Yuri, T. Hisamatsu, K. Watanabe, Y. Etori, Trans. ASME J. Eng. Gas Turb. Power 119 (1997) 506.
[6] K. Aoyama, S. Mandai, Trans. ASME J. Eng. Gas Turb. Power 106 (1984) 795.
[7] Y. Tochihara, Y. Ozawa, presented at the Fourth International Workshop on Catalytic Combustion, San Diego, CA, USA, 14–16 April, 1999.
[8] W.J. Kuper, M. Blaauw, F. van der Berg, G.H. Graaf, Catal. Today 47 (1999) 377.
[9] R.A. Dalla Betta, J.C. Schlatter, S.G. Nickolas, D.K. Yee, T. Shoji, ASME Paper No. 94-GT-260 (1994).